Chemical Engineering Journal 253 (2014) 130–137

Contents lists available at ScienceDirect

Chemical Engineering Journal

journal homepage: www.elsevier.com/locate/cej

Design and synthesis of pyrophosphate acid/graphene composites with wide stacked pores for methylene blue removal

Chubei Wang [a,*], Jianwei Zhou [a], Jun Ni [b], Yuliang Cheng [c], Hui Li [c]

[a] Institute of Energy and Fuel, Xinxiang University, Xinxiang, Henan 453003, China
[b] National Engineering Research Center of Chemical Fertilizer Catalyst, Fuzhou University, Fuzhou, Fujian 350002, China
[c] Department of Life Sciences and Technology, Xinxiang University, Xinxiang, Henan 453003, China

HIGHLIGHTS

- Stacked pore size is noticeably improved by aggregation of functionalized sheets.
- The average interlayer spacing of the product is wider than that of RGO.
- Modified graphene has high adsorption capacity for methylene blue.

GRAPHICAL ABSTRACT

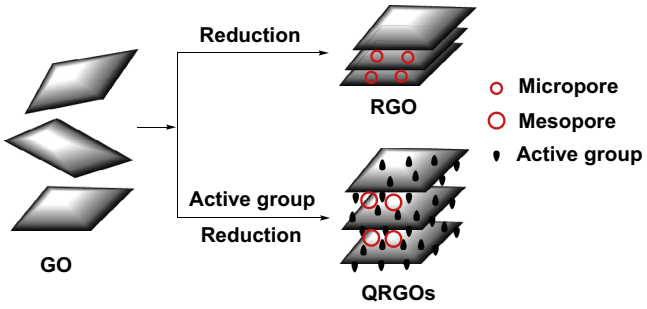

ARTICLE INFO

Article history:
Received 6 March 2014
Received in revised form 3 May 2014
Accepted 5 May 2014
Available online 20 May 2014

Keywords:
Graphene
Porosity
Adsorption
Methylene blue

ABSTRACT

Pyrophosphate acid/graphene composites were prepared by using graphite oxide and phosphorus trichloride as raw materials. Phosphorus-based groups and residual oxygenated functional groups may reduce graphene sheet restacking to form graphite. The stacked pore size and binding site of the composites are noticeably improved by aggregation of functionalized sheets. The average interlayer spacing of the composites is wider than that of reduced graphene oxide (RGO). Compared with the high surface area of the adsorbent, the porosity and pore size of the materials exert significantly greater influence on the adsorption capacity of the composites. The adsorption process follows second-order rate. The adsorption of methylene blue preferably fitting the Langmuir adsorption isotherm suggests monolayer coverage of adsorbed molecules. The adsorption capacity of the composites for methylene blue is 200.0 mg g^{-1}, which is significantly higher than those of RGO (80.0 mg g^{-1}) and active carbon (46.7 mg g^{-1}).

1. Introduction

Organic dyes have been ubiquitously utilized in leather, paper, rubber, and textile industries. However, the discharge of this wastewater into streams results in serious environmental pollution because of their resistance to decomposition [1–3]. Considerable effort has been exerted to remove these organic pollutants either through catalytical decomposition or physicochemical adsorption. For example, various semiconductor nanocrystals, such as TiO_2, $BiNbO_4$, $AgTaO_3$, and $BiTaO_3$, have been extensively investigated to photocatalytically decompose organic compounds [4–8]. Several adsorbents, such as silica [9,10], active carbon [11], resin [12], and halloysite nanotubes [3], have been widely studied to remove organic compounds by physical and/or chemical adsorption. However, the exploration of novel materials and techniques for highly efficient and economical removal of organic pollutants from industrial effluents is still of great interest.

* Corresponding author. Tel./fax: +86 373 3682028.
E-mail address: wangchubei@163.com (C. Wang).

http://dx.doi.org/10.1016/j.cej.2014.05.020
1385-8947/

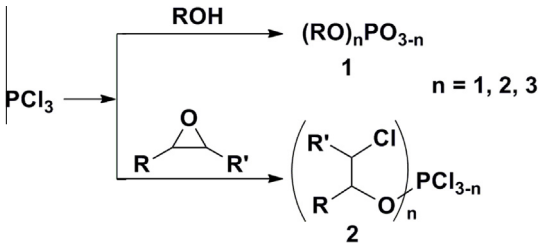

Fig. 1. PCl_3 reaction with OH groups and epoxy bonds.

Mesoporous materials with regular geometry have elicited considerable attention because of their high potential in practical applications, such as catalysis [13–14], adsorption [15–17], and separation [18–19]. Other materials with irregularly shaped pores have high surface area, high pore volume, tunable pore size, wide porosity distribution, and more binding sites. An example of these materials is graphene. However, graphene has low adsorption capacity. The pore size of graphene limits the transfer of adsorbates from the adsorbent surface into the pores, and the low pore volume of this material results in a few occupied pores [20]. These pores are not found on the sheets but are instead formed by sheet aggregation. These materials contain one or several micropores, mesopores, and macropores. Zhang et al. [21] found that some hybrid composites could form porous structures. Some groups attached on graphene sheets act as spacers [22–28] that improve pore size distribution during aggregation. Moreover, adsorbent functionalization has significantly expanded the adsorption capacity of pure ones [29–31]. This method is practical for the development of highly efficient adsorbents through grafting or incorporation of special groups and binding sites on graphene sheets. Adding these active groups on graphene sheets might not only reduce as-reduced graphene sheet restacking to form graphite but also improve pore size distribution and increase adsorption capacity. To the best of our knowledge, only a few studies have attempted to improve adsorption capacities for porous adsorbents by the aggregation of graphite sheets.

This work reports a one-pot method for the synthesis of pyrophosphate acid/graphene composites, namely, quasi-reduced graphene oxides (QRGOs). QRGOs were prepared by substituting GO with PCl_3 and by employing thermal reduction. As illustrated in Fig. 1, PCl_3 mainly reacted with OH and epoxy groups to form compounds **1** and **2**, respectively [32,33]. These compounds reacted with water to form phosphite or phosphate acids. The resulting QRGOs have wider pore size and more binding sites than RGO, and the composites exhibit excellent scavenging capability for methylene blue (MB).

2. Materials and methods

2.1. Materials

Pristine graphite was purchased from Qingdao BCSM Co., Ltd., (Qingdao, China), and phosphorous trichloride (PCl_3) was supplied by Shanghai Chemical Reagent Company (Shanghai, China). All other chemicals were of analytical grade and were purchased from Beijing Chemical Reagents Company (Beijing, China). All chemicals were used without further purification.

2.2. Synthesis of QRGOs, control sample, and RGO

A mixture of GO (1.00 g) and acetonitrile (40 mL) was sonicated for 30 min. Water bath sonication was performed using a JL-60 DTH sonicator (100 W). PCl_3 (6 mL) was added to the GO solution at −5 °C under stirring for 1 h. Water (3 mL) was added, and the mixture was heated and refluxed for 7 h. The mixture was poured in water (100 mL), and the product was collected by filtration and washed several times with deionized water. The QRGOs were dried at 50 °C for 10 h to yield a loose black powder (0.94 g).

The control sample was prepared under a similar process without PCl_3.

GO (0.20 g) was dispersed in water (500 mL) with the aid of ultrasonication, and then hydrazine hydrate (80 wt%, 20 mL) was added at 100 °C for 24 h [34–36]. The product was collected by filtration and washed several times with deionized water. The RGO was dried at 50 °C for 10 h to yield a loose black powder (0.12 g).

2.3. Characterization of QRGOs

Fourier-transform infrared (FTIR) spectra were obtained on an FTS-40 (Bio-Rad, CA, USA). Raman spectra were recorded on a Renishaw InVia multi-channel confocal microspectrometer with 532 nm excitation laser. X-ray diffraction (XRD) measurements were obtained on an X'pert PRO diffractometer using Co Kα radiation. X-ray photoelectron spectroscopy (XPS) with monochromatized Al Kα X-ray ($h\nu$ = 1486.6 eV) radiation (ThermoFisher Scientific Co., ESCALAB 250, USA) was used to investigate the surface properties of the QRGOs. The shift in binding energies was corrected using the C 1s signal at 284.6 eV as the internal standard. Scanning electron microscopy (SEM) and energy-dispersive X-ray (EDX) spectroscopy were performed using Hitachi S-4800 field emission and FEI-Quanta 200 scanning electron microscopes, respectively. High-resolution TEM (HRTEM) was performed on a JEOL JEM-2011 electron microscope operated at 200 kV, equipped with an Oxford Link ISIS energy dispersive X-ray spectroscopy (EDX) system, and a Gatan 794 camera. Nitrogen sorption measurements were performed with ASAP 2020 V3.01H (Micromeritics, USA). Specific surface areas, pore volumes, and pore size distributions were calculated using the Brunauer–Emmett–Teller (BET) and density functional theory (DFT) models from the

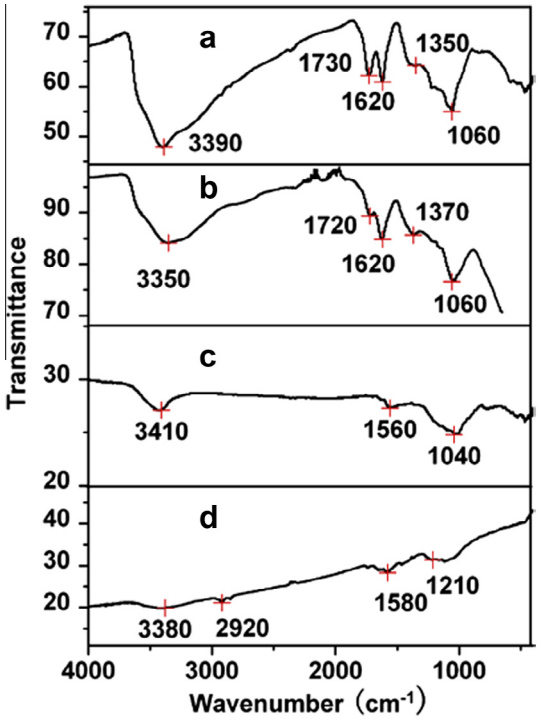

Fig. 2. FTIR spectra of GO (a), control sample (b), RGO (c), and QRGOs (d).